Measurement of Condensed Water Content in Liquid and Ice Clouds Using an Airborne Counterflow Virtual Impactor

CYNTHIA H. TWOHY, ALLEN J. SCHANOT, AND WILLIAM A. COOPER

*National Center for Atmospheric Research, Boulder, Colorado**

2 April 1996 and 22 July 1996

ABSTRACT

Condensed water content (CWC) measured using a counterflow virtual impactor (CVI) with a Lyman-α hygrometer downstream is compared with that measured by other airborne instruments (a hot-wire probe, a PMS FSSP, and a PMS 2D-C). Results indicate that the CVI system provides a reliable measurement of CWC in both liquid- and ice-phase clouds and that the CVI measures CWC contained in both large and small hydrometeors; this means that the condensed water present in both phases and virtually all hydrometeor sizes can be measured with a single device. Small ice contents of a few milligrams per cubic meter present in cirrus clouds can also be measured by the technique.

1. Introduction

The distribution of liquid water and ice in clouds is germane to many problems facing the atmospheric science community today; in fact, water in all its forms might be considered the most significant substance in the atmosphere. Water interacts with both longwave and shortwave radiation in the atmosphere, and knowledge of the phase and spatial distribution of water is necessary in order to understand its effect on climate. Water is also important in cloud physics and dynamics, where the amount of liquid and ice provides information about the extent of condensation, entrainment, and precipitation occurring in clouds. The magnitude of CWC and how it is apportioned to droplets or ice within clouds also governs the extent and nature of chemical reactions within clouds, and ultimately, how efficiently chemical species are removed from the atmosphere.

The vertical and horizontal inhomogeneity of clouds means that mobile platforms, such as aircraft, are needed to address many aspects of these problems. Remote sensing techniques (e.g., Greenwald et al. 1993) are useful but may have insufficient resolution and still require in situ validation. The measurement of CWC from aircraft can be problematic, however, as standard instruments do not measure accurately or reliably in all cloud types. Instruments routinely used on aircraft for CWC measurement fall into two fundamental types: optical devices that employ the interaction of cloud particles with light, and heated devices that utilize the cooling that occurs as droplets evaporate upon striking a hot element. The major advantages and disadvantages of these different methods are summarized below.

The most commonly used optical instruments (Knollenberg 1981) are manufactured by Particle Measuring Systems (PMS). The forward-scattering spectrometer probe (FSSP) sizes individual particles using Mie scattering theory, while the optical array probes (2D-C and 2D-P) save a two-dimensional image for analysis. The PMS probes have a fast response, and when several of the PMS probes are used together, the entire cloud particle size distribution can be measured. The 2D probes measure larger particles and can be used to determine whether they are composed of ice or liquid. The size distribution measured by the FSSP-100 is frequently integrated to obtain cloud liquid water content. This method engenders a large uncertainty, about 100% without corrections and 55% with corrections (Baumgardner et al. 1990), although Hoppel et al. (1994) suggested errors as large as 240% can occur. Uncertainty increases when ice crystals are present (Gardiner and Hallett 1985).

The CSIRO King probe (King et al. 1981) uses a heated wire to measure liquid water content (LWC). This instrument is relatively simple and accurate ($\approx$ 15%) for higher LWC; however, accuracy is diminished at lower LWC since the baseline (the clear-air signal upon which the in-cloud signal is superimposed) is dependent on airspeed, temperature, and pressure (Heymsfield and Mil-

* The National Center for Atmospheric Research is sponsored by the National Science Foundation.

Corresponding author address: Dr. Cynthia H. Twohy, Research Aviation Facility, NCAR—Atmospheric Technology Division, P.O. Box 3000, Boulder, CO 80307-3000.

oshevich 1989). While droplets between 5- and 40-μm diameter are efficiently sampled by the CSIRO probe (King et al. 1981), ice particles do not adhere and so are not detected.

This paper describes and evaluates one relatively new method, a counterflow virtual impactor (CVI) used in series with a Lyman-α hygrometer, for airborne measurement of CWC. Different versions of the CVI have been used to measure CWC previously (e.g., Ogren et al. 1989; Noone et al. 1993; Ström and Heintzenberg 1994), but little comparison with other techniques has been presented. Here CVI measurements taken on the National Center for Atmospheric Research (NCAR) Electra aircraft are compared to measurements made by a hot-wire probe and PMS optical probes in clouds containing both supercooled water and ice crystals. The uncertainty of the CVI measurement is also estimated.

2. Principle of CVI operation

Inside the CVI inlet, cloud particles (either liquid or ice) moving with the aircraft velocity are impacted into an initially dry airstream. Volatile components that evaporate within the heated inlet, as well as nonvolatile residual particles, are conveyed to instruments in the aircraft cabin. Various characteristics of the cloud particles can subsequently be analyzed, but we focus here on measurement of water vapor from the evaporated cloud particles with a Lyman-α hygrometer. This is then used to derive cloud CWC. The CVI method has several advantages.

1) The counterflow air out through the tip of the CVI inlet prevents ambient water vapor from being collected and permits only condensed-phase cloud particles, which have higher inertia, to enter the inlet where they are impacted into desiccated air.
2) The CVI inlet tip is maintained at about 50°C, so supercooled or ice clouds can be sampled as well as warm clouds.
3) The minimum size of a cloud particle able to enter the inlet tip is dependent on particle velocity, inlet size, and CVI counterflow rate, which can be adjusted in flight to change the size of particles collected. Ice crystals and liquid droplets can both be sampled, as long as they are of sufficient size. Calculated impaction efficiency has been shown to agree with measurements (Noone et al. 1988; Anderson 1992). The "cut size," or minimum particle diameter collected with 50% efficiency, is about 7-μm aerodynamic diameter (diameter of a unit-density sphere) for the NCAR CVI at sea level but can be increased as desired.
4) The condensed water contained in the entire size spectrum, up to drizzle-sized drops and large ice crystals, can be measured accurately.
5) Approximately 150 L min^{-1} of air is swept out by the CVI tip, but cloud particles in this volume are injected into a much smaller flow (typically 8 L min^{-1}) within the CVI probe, so CWC is enhanced within the CVI. This leads to more accurate detection of low CWC. The CVI enhancement factor is calculated by dividing the two flow rates (e.g., 150/8, leading to a 19-fold enhancement in this example).

3. Experiment

The CVI was flown on the NCAR Electra during the Winter Icing and Storms Project (WISP) in February and March of 1994. The study focused on the development of ice in orographic wave clouds and upslope or winter storms. Sampling was conducted under a variety of conditions throughout the project, so clouds consisting of all liquid, all ice, and mixed phases were encountered. Data are presented here from one winter storm flight and from two wave cloud flights.

The CVI inlet was mounted on top of the fuselage, 46 cm from the aircraft skin, at fuselage station 215 (approximately 5.54 m aft of the radome nose). The sensor used to measure water vapor in the CVI sample stream was a Lyman-α hygrometer (Buck 1985), which measures absorption of Lyman-α radiation (121.56 nm) by water vapor. Although this sensor has well-known problems with electronic drift (Schanot 1990), it measures at a high rate over a broad range of concentrations. To minimize the impact of drift on these measurements, the Lyman-α was mounted in the heated cabin in series with a General Eastern chilled-mirror hygrometer (NCAR model 1101B), and the signals were coupled using the method of Schanot (1990). Condensed water contents presented here were calculated by first subtracting the water vapor content inside the CVI just prior to cloud entry from the in-cloud measurement, and then dividing the result by the CVI enhancement factor.

4. Results

Figure 1 shows data taken during a 30-min sampling of a storm system that formed east of the Rocky Mountains on 8 February 1994. For about the first 5 min and the last 15 min shown here, the aircraft was "porpoising" up and down through the top of the storm, while a level leg was flown near the cloud top during the intervening period. The temperature within the cloud was about -18°C. One minute in time on the abscissa represents about 6 km in horizontal extent.

The top trace is CWC (g m^{-3}) in droplets larger than 11-μm diameter measured by the CVI, the second is CWC measured by a CSIRO hot-wire probe, the third is CWC derived from the FSSP-100 size distribution (2–52 μm), and the fourth is the voltage output from the Rosemount icing detector (Brown 1982). As supercooled droplets strike and freeze on the Rosemount sensor, the oscillation frequency changes proportionally to the mass of the adhering droplets. The large voltage

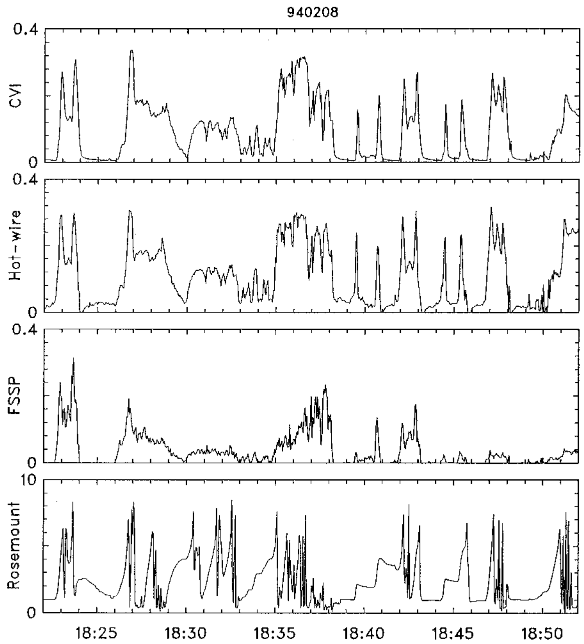

FIG. 1. Condensed water content as a function of time (UTC) measured during a winter storm on 8 February 1994. The top trace is from the CVI, the second is from the CSIRO King hot-wire probe, the third is from the FSSP-100, and the fourth is from the Rosemount icing detector. All units are in grams per cubic meter except for the Rosemount, which is in volts.

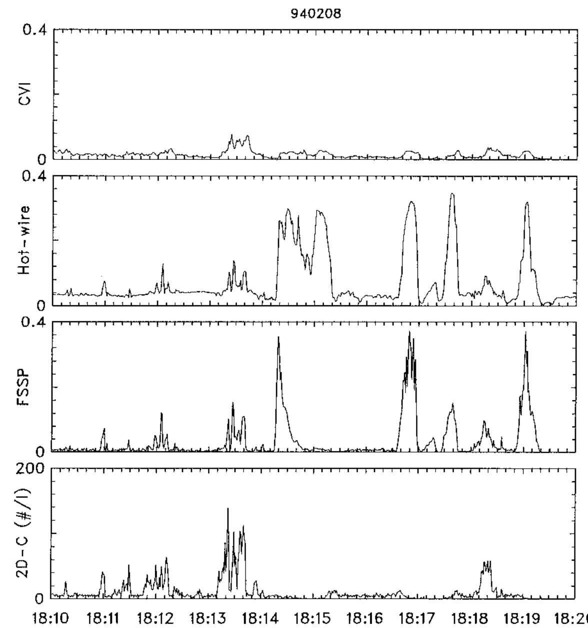

FIG. 2. Condensed water content as a function of time measured during a winter storm on 8 February 1994. The top trace is from the CVI set at a 20-μm cut size, the second is from the CSIRO King hot-wire probe, the third is from the FSSP-100, and the fourth is number concentration from the PMS 2D-C probe. All units are grams per cubic meter except for the 2D-C, which is in units per liter.

drops occur when the sensor reaches its maximum capacity and the frozen water is shed. (Ice crystals measured by the PMS 2D-C probe were neglected here since they were not large and their concentration was only a few per liter—numbers too small to contribute significantly to CWC.)

Supercooled water actually accreted as ice on the arms of the FSSP probe during this flight, and as a result its CWC measurements are unreliable and often much lower than the CVI and hot-wire values. The Rosemount sensor has been used by Heymsfield and Miloshevich (1989) to quantify liquid water content, but the large number of deicing events during this time period make it impractical to derive a LWC time series by this method. In this case, the CVI is compared to the hot-wire probe, which is accurate and reliable in supercooled water. Excellent agreement is observed between these two instruments, although the CVI lags behind the hot-wire due to the approximately 2-s transport time for water vapor through the CVI sample tubing. Regression of the hot-wire against the CVI using a 2-s lag of the hot-wire data produced the following relationship: $\mathrm{CWC}_{\text{hot-wire}} = 1.05\mathrm{CWC}_{\mathrm{CVI}} + 0.01$, with $r^2 = 0.94$. This comparison verifies that the CVI efficiently measures LWC in supercooled clouds.

Figure 2 shows another time period of the same flight, except the minimum CVI cut size has been increased to about 20-μm diameter. After 1814 UTC, the hot-wire and FSSP traces are similar to those in Fig. 1, but the CVI CWC is nearly an order of magnitude less. This indicates that only about 10% of the total CW is contained in droplets or crystals larger than 20-μm diameter and demonstrates the size-selective capability of the CVI. The bottom trace in Fig. 2 displays the concentration (L^{-1}) of ice crystals in the diameter range 25–800 μm measured by a 2D-C probe. Between 1813 and 1814 UTC, the liquid water measured by the hot-wire is much lower and the number of ice crystals measured by the 2D-C is higher; the CVI data also show this shift in partitioning between hydrometeor sizes and demonstrate that for this time period the magnitude of CW contained in the large crystals is similar to that contained in the smaller droplets.

Figure 3 shows ice water contents measured by the CVI (cut size: 11 μm until 2158:35 UTC when it was increased to 20 μm) in a series of passes through wave clouds on 3 February 1994 at temperatures of about -40°C. Although some liquid water can still exist in very small droplets at this temperature (e.g., Heymsfield and Miloshevich 1993), most of the condensed water mass is expected to be contained in ice. The CVI indicates a regular wave structure with peak CWCs of about 0.1 g m^{-3}. The hot-wire probe (and the Rosemount icing detector, not shown) shows only a slight perturbation that is correlated with temperature and pressure changes, as expected if only ice were present. Although the FSSP data can be difficult to interpret when ice is present (Heymsfield and Miloshevich 1989), the FSSP-

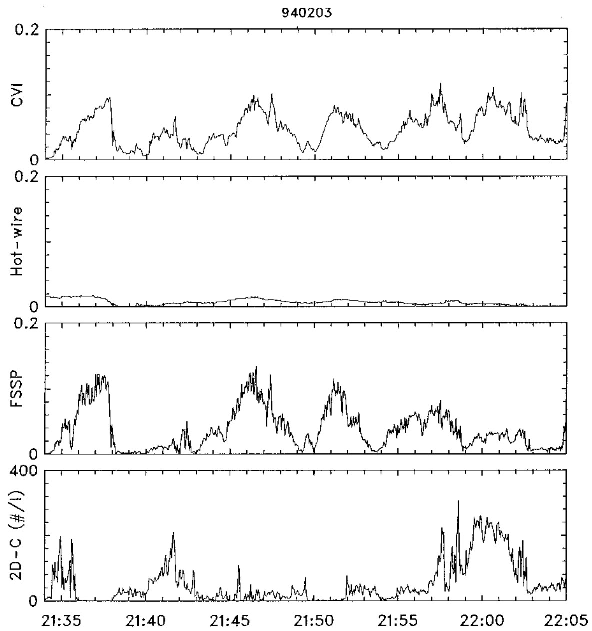

FIG. 3. Condensed water content as a function of time measured in a mountain wave cloud on 3 February 1994. The top trace is from the CVI, the second is from the hot-wire probe, the third is from the FSSP-100, and the fourth is number concentration from the PMS 2D-C probe. All units are grams per cubic meter except for the 2D-C, which is in units per liter.

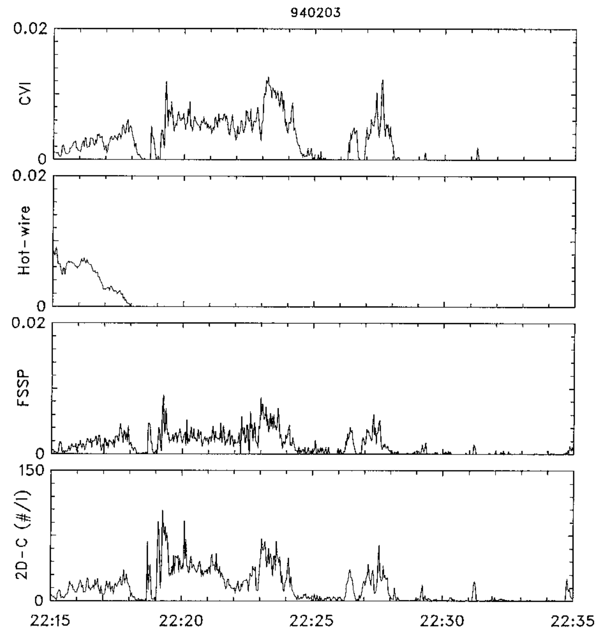

FIG. 4. Condensed water content as a function of time measured in a mountain wave cloud on 3 February 1994 (at a higher altitude than in Fig. 3). The top trace is from the CVI, the second is from the hot-wire probe, the third is from the FSSP-100, and the fourth is number concentration from the PMS 2D-C probe. All units are grams per cubic meter except for the 2D-C, which is in units per liter.

derived condensed water content (third plot) is similar in magnitude to the CVI CWC. The CVI and FSSP CWC disagree substantially only when significant numbers of large ice crystals (>50 μm) are present, as evidenced by the 2D-C data; between 2140 and 2142 and between 2157 and 2203 UTC, the CVI measures the additional water mass present in large crystals. Linear regression using data from the intervening period (2143:00–2156:30) produced the following relationship: $CWC_{FSSP} = 1.24\ CWC_{CVI} - 0.01$, with $r^2 = 0.83$. Since the density and scattering characteristics of the ice crystals were not known precisely, no special processing was used for the FSSP data (i.e., liquid water spheres were assumed). However, a very simple correction could be made to the CWC_{FSSP} by multiplying by 0.917 (density of solid ice), in which case the ratio of CWC_{FSSP} to CWC_{CVI} would drop to 1.14.

The next data shown (Fig. 4) were also obtained in wave clouds on 3 February, but sampling occurred at a higher altitude and lower temperature (−46°C), where no cloud was visually apparent. The wave structure still persists at this altitude, although the CWC is lower by an order of magnitude. Again, the FSSP tracks the CVI quite well, although the FSSP CWC measurement is considerably lower than the CVI ($CWC_{FSSP} = 0.44\ CWC_{CVI} - 0.01$, with $r^2 = 0.76$). This difference may represent the actual CWC present in large ice crystals, which are more numerous than in the previous time period and would be measured by the CVI, but not by the FSSP. These data are especially encouraging, because they verify the promise of the CVI technique for measurement of the very low ice contents (on the order of a few milligrams per cubic meter) in cirrus clouds.

Calculation of ice water content from the 2D images is a highly uncertain procedure due to the third-power dependence on particle size and the variety of crystal sizes, habits, and densities that may be present. However, it is still of interest to compare the CVI CWC to this method. Unfortunately, the 2D-C probe used on 3 and 8 February had a bit set incorrectly, introducing a substantial error in particle sizing. 2D-C CWC was therefore calculated for a randomly selected time period of a later flight (4 March) in a cold wave cloud (−35°C) when this problem was fixed. The amount of condensed water contained in each crystal was derived using a relationship observed for solid thick plates (Davis 1974) of $CWC = 0.0807D^{2.778}$, where D is the maximum dimension in centimeters. Although the exact crystal habit was not determined, this compact crystal relationship should be fairly representative of the small crystals observed. We estimate a factor of 2 error is possible, however, based on the range of mass–dimension relationships presented by Davis (1974). Integrated CWCs were smoothed with a 6-s running average due to the high sampling frequency (often several samples per second). Figure 5 shows that the two signals track quite well and agree within the expected uncertainty.

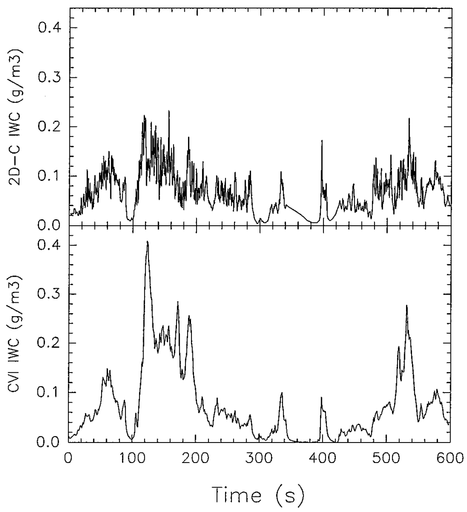

FIG. 5. Condensed water content measured in a cold wave cloud on 4 March 1994 between 2040 and 2050 UTC. Top trace is from the PMS 2D-C probe and bottom is from the CVI.

5. Uncertainty

The primary source of random error in CWC measured by the CVI is electronic drift, estimated at about 5% of the signal when the Lyman-α is within the heated aircraft cabin and coupled to the GE dewpoint measurement. Bias errors are contributed by the uncertainty in calculation of the enhancement factor inside the CVI, estimated at 10%, and knowledge of the varying water vapor baseline. With careful processing, the latter error is about 0.002 g m^{-3}, or 1% for a CWC of 0.2 g m^{-3} and 10% for a CWC of 0.02 g m^{-3}. Combination of the errors by the root-sum-square (RSS) method leads to an 11% uncertainty for a CWC of 0.2 g m^{-3} and a 15% uncertainty for 0.02 g m^{-3}. This contrasts quite favorably with uncertainties in CWC measured by PMS probes of more than 50% (Baumgardner et al. 1990).

A more stable baseline would add to the utility of this technique for measuring the low CWCs present in cirrus clouds. This baseline is largely determined by the amount of moisture in the air that is pumped to the CVI inlet (into which cloud particles are impacted). This air is currently provided by taking ambient air from the aircraft cabin and passing it through a silica gel desiccant. The impaction air humidity thus varies strongly with the cabin humidity, as well as with the efficiency of the desiccant at the time of the measurement. Improvements planned for cirrus studies include a dry air cylinder for the air source to the CVI inlet, and the substitution of a dual-path, dual-wavelength ultraviolet hygrometer (Weinheimer and Schwiesow 1992), under development at NCAR, for the standard Lyman-α. With these improvements, we expect to minimize the variability in the clear-air baseline and lower the RSS uncertainty to about 10% even for very low CWCs.

The above uncertainty analysis assumes that the CVI inlet is located in a region where particle trajectories are not disturbed by the aircraft itself. Depending on location and the actual particle size distribution, errors as large as a factor of 2 in CWC could easily result due to a deficit or enhancement of certain particle sizes at the sampling location (e.g., Twohy and Rogers 1993). Thus the selection of a suitable location, or at least modeling that predicts changes in the size distribution at the sampling location, is essential if uncertainties in any CWC measurement technique are to be minimized.

6. Conclusions

A preliminary comparison of condensed water content measured using the CVI–Lyman-α combination with that measured using other techniques indicates that the CVI functions as expected in a variety of cloud types. The CVI has the advantage of being able to measure water in both the liquid and ice phases, even the larger crystals detected by PMS 2-D probes; this single device that can measure CWC across the entire spectrum of hydrometeor types and sizes should ease data analysis and minimize uncertainty inherent in combining measurements from different instruments. Uncertainty for CWC measured by the CVI technique is estimated to be about 11% for a CWC of 0.2 g m^{-3} but increases for smaller CWC. Planned improvements include an ultraviolet hygrometer for water vapor detection and the addition of a dry air cylinder to provide air to the inlet tip. These modifications will provide accurate measurements of CWC down to at least a few milligrams per cubic meter, making the CVI particularly useful for cirrus cloud studies.

Acknowledgments. Thanks to Dave McFarland of NCAR's Research Aviation Facility, who contributed to the use of the Lyman-α hygrometer, and to the pilots of the NCAR Electra. Tad Anderson of the University of Washington helped characterize the CVI inlet. Bob Charlson, Jost Heintzenberg, and John Ogren were originators of the CVI concept.

REFERENCES

Anderson, T. L., 1992: Optimization of a counterflow virtual impactor (CVI) for studying aerosol effects on cloud droplet number. Ph.D. dissertation, University of Washington, 232 pp. [Available from University Microfilms, 300 North Zeeb Rd., Ann Arbor, MI 48106.]

Baumgardner, D., W. A. Cooper, and J. E. Dye, 1990: Optical and electronic limitations of the forward-scattering spectrometer probe. *Liquid Particle Size Techniques,* Vol. 2, ASTM STP 1083, E. D. Hirleman, W. D. Bachalo, and P. G. Felton, Eds., American Society for Testing and Materials, 115–127.

Brown, E. N., 1982: Ice detector evaluation for aircraft hazard warning and undercooled water content measurements. *J. Aircr.,* **19,** 980–983.

Buck, A., 1985: The Lyman-alpha hygrometer. *Moisture and Humidity: Measurement and Control in Science and Industry, Proc. 1985 Int. Symp. on Moisture and Humidity,* Washington, DC, Instrument Society of America, 411–436.

Davis, C. I., 1974: The ice-nucleating characteristics of various AgI aerosols. Ph.D. dissertation, University of Wyoming, 267 pp. [Available from University of Wyoming, Dept. of Mechanical Engineering, Laramie, WY 82071.]

Gardiner, B. A., and J. Hallett, 1985: Degradation of in-cloud forward scattering spectrometer probe measurements in the presence of ice particles. *J. Atmos. Oceanic Technol.,* **2,** 171–180.

Greenwald, T. J., G. L Stephens, T. H. Vonder Haar, and D. L. Jackson, 1993: A physical retrieval of cloud liquid water over the global oceans using Special Sensor Microwave/Imager (SSM/I) observations. *J. Geophys. Res.,* **98,** 18 471–18 488.

Heymsfield, A. J., and L. M. Miloshevich, 1989: Evaluation of liquid water measuring instruments in clouds sampled during FIRE. *J. Atmos. Oceanic Technol.,* **6,** 378–388.

——, and ——, 1993: Homogeneous ice nucleation and supercooled liquid water in orographic wave clouds. *J. Atmos. Sci.,* **50,** 2235–2253.

Hoppel, W. A., G. M. Frick, J. W. Fitzgerald, and R. E. Larson, 1994: Marine boundary layer measurements of new particle formation and the effects nonprecipitating clouds have on aerosol size distribution. *J. Geophys. Res.,* **99,** 14 443–14 459.

King, W. D., C. T. Maher, and G. A. Hepburn, 1981: Further performance tests on the CSIRO liquid water probe. *J. Appl. Meteor.,* **20,** 195–202.

Knollenberg, R. G., 1981: Techniques for probing cloud microstructure. *Clouds, Their Formation, Optical Properties and Effects,* P.V. Hobbs and A. Deepak, Eds., Academic Press, 15–85.

Noone, K. B., K. J. Noone, J. Heintzenberg, J. Ström, and J. A. Ogren, 1993: In situ observations of cirrus cloud microphysical properties using the counterflow virtual impactor. *J. Atmos. Oceanic Technol.,* **10,** 294–303.

Noone, K. J., J. A. Ogren, J. Heintzenberg, R. J. Charlson, and D. S. Covert, 1988: Design and calibration of a counterflow virtual impactor for sampling of atmospheric fog and cloud droplets. *Aerosol Sci. Technol.,* **8,** 235–244.

Ogren, J. A., J. Heintzenberg, A. Zuber, K. J. Noone, and R. J. Charlson, 1989: Measurements of the size-dependence of nonvolatile aqueous mass concentrations in cloud droplets. *Tellus,* **41B,** 24–31.

Schanot, A., 1990: An evaluation of the uses and limitations of a Lyman-alpha hygrometer as an operational airborne humidity sensor. Preprints, *Sixth Symp. on Meteorological Observations and Instrumentation,* New Orleans, LA, Amer. Meteor. Soc., 257–260.

Ström, J., and J. Heintzenberg, 1994: Water vapor, condensed water, and crystal concentration in orographically influenced cirrus clouds. *J. Atmos. Sci.,* **51,** 2368–2383.

Twohy, C. H., and D. Rogers, 1993: Airflow and water-drop trajectories at instrument sampling points around the Beechcraft King Air and Lockheed Electra. *J. Atmos. Oceanic Technol.,* **10,** 566–578.

Weinheimer, A. J., and R. Schwiesow, 1992: A two-path, two-wavelength ultraviolet hygrometer. *J. Atmos. Oceanic Technol.,* **9,** 407–419.